(8) Hashimoto, T.; Tsukahara, J.; Kawai, H. *Macromolecules* **1981**, *14*, 708.
(9) Preliminary results in our laboratory (by T. Ougizawa et al.).
(10) Note that the annealing conditions are identical with those of the longest case in Figure 4, at which the scattering peak has disappeared.
(11) Kambour, R. P.; Bendler, J. T.; Bopp, R. C. *Macromolecules* **1983**, *16*, 753.
(12) ten Brinke, G.; Karasz, F. E.; MacKnight, W. J. *Macromolecules* **1983**, *16*, 1827.
(13) Paul, D. R.; Barlow, J. W. *Polymer* **1984**, *25*, 487.
(14) The B unit in BR is different from that in SBR. The B unit in BR is cis-1,4 (solution polymerization). On the contrary, B units in SBR are composed of cis-1,4 (13%), trans-1,4 (69%), and vinyl (18%) (emulsion polymerization). B in SBR (=B′) ≠ B in BR. That is, our system is (B homopolymer)/(B′S random copolymer).

Toshiaki Ougizawa, Takashi Inoue,* and Hans W. Kammer

Department of Textile and Polymeric Materials
Tokyo Institute of Technology
Ookayama, Meguro-ku, Tokyo 152, Japan

Received June 13, 1985

Direct Observations of Macroperoxyl Radical Propagation and Termination by Electron Spin Resonance and Infrared Spectroscopies†

Numerous investigations have been made of the behavior of peroxyl radicals in oxidizing polymers.[1-8] These studies have depended heavily on the use of electron spin resonance (ESR) spectroscopy, which has great sensitivity for free radical species. However, the method is blind to nonradical species, which, in fact, constitute the bulk of the oxidation products. Nevertheless, the ESR observation of the decay of peroxyl radicals ($PO_2\cdot$) under vacuum to form macroalkyl radicals has been cited as direct evidence for the peroxyl propagation reaction 1.[1,2,5,7] In addition

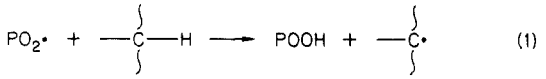

(1)

the conversion of an initially ^{17}O-labeled peroxyl population to ^{16}O peroxyl radicals in an $^{16}O_2$ atmosphere has been suggested to be definitive for this propagation (sequence 2).[6] Although, many of these studies refer to polypropylene (PP), both ESR methods ignore the very real possibility of macroalkyl formation without the intermediacy of the propagation step (reaction 1). This can result from *tert*-peroxyl self-reactions (reaction 3), which occur

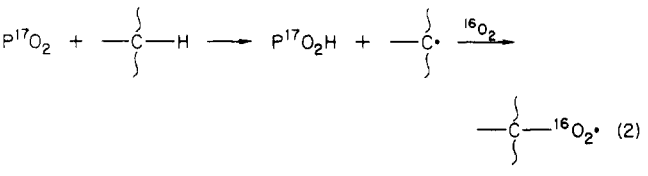

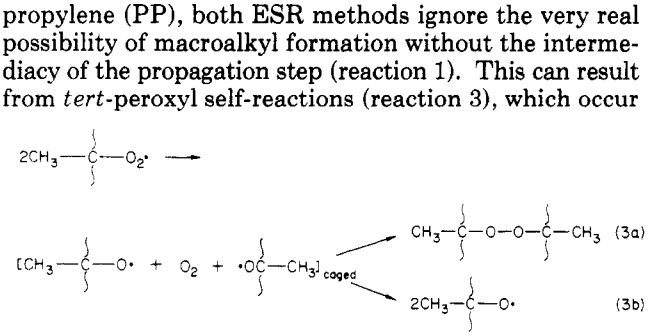

with a high probability in the early life of a radical pair or cluster.[3,5] As well as dimerization to give a peroxide cross-link, the reactive macroalkoxyl radicals produced in *tert*-peroxyl self-reaction are expected to either hydrogen abstract from the polymer to form macroalkyl radicals or undergo β-scission to form macroalkyl radicals (reaction 4). In both these cases these macroalkyls will then combine with O_2 to re-form peroxyls.

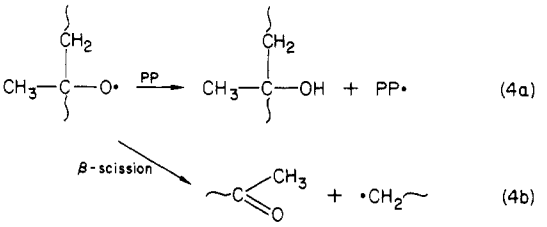

(4a) (4b)

Other evidence for the occurrence of the oxidative propagation steps (reaction sequence 2) in solid polymers comes from the indirect method of product analysis after appreciable oxidation.[3,4] In an attempt to obtain more direct evidence for the behavior of macroperoxyl radicals (both propagation and termination) and to resolve the potential ambiguity in the ESR approach, we have combined ESR and Fourier transform infrared (FTIR) spectroscopy to study both the decay of the polypropylene peroxyl ($PPO_2\cdot$) population and the associated formation of oxidation products. Although FTIR lacks the sensitivity of ESR, relatively high concentrations of $PPO_2\cdot$ can be generated by the γ-irradiation of PP in the presence of O_2 at −78 °C, conditions under which these radicals can neither propagate nor terminate. If these $PPO_2\cdot$ radicals are then allowed to propagate and terminate by suddenly warming above the PP T_g, we have found it possible to record the IR spectra of oxidation products as they accumulate from time zero. De Vries et al. have previously combined ESR and FTIR in the study of polyethylene oxidation but only reported the radical level at 77 K immediately after γ-irradiation and measured a single spectrum of the oxidized polymer after storage at room temperature, ignoring the decay process.[8]

Isotactic PP film (iPP, ~30-μm thickness unoriented, Hercules resin, exhaustively extracted to remove processing additives) and ~50 mg of pellets of atactic PP (aPP, Gulf resin, reprecipitated from toluene) or aPP coatings (~140 μm) on one surface of NaCl disks were exposed in an AECL Gamma cell 220 (^{60}Co, 1.35 Mrd·h^{-1}). During irradiation, the tubes containing PP samples in O_2 or air were refrigerated at −78 °C in solid carbon dioxide. The ESR spectra were recorded on prerolled scrolls of iPP film or on the aPP pellets after transfer at 77 K to fresh (color-center free) ESR tubes. The spectrometer was a Varian E4, equipped with a Nicolet 1170 integration system which was standardized both with an in-cavity ruby signal and known quantities of 2,2-diphenyl-1-picrylhydrazyl solution. Peroxyl signals were quantified at 10-mW microwave power (well below the saturation limit) but signals from macroalkyl-containing samples were found to require ≤1.0 mW to prevent detector saturation. Some aPP pellets showed a residual macroalkyl ESR signal immediately after irradiation in air in addition to the expected the $PPO_2\cdot$ signal, and were held at −78 °C until O_2-diffusion converted these radicals to $PPO_2\cdot$. At the dose rate used, all iPP films showed only a $PPO_2\cdot$ ESR signal.

FTIR spectra were recorded on separately irradiated iPP film samples (clamped flat in five layers on aluminum frames) and on the aPP-coated NaCl disks. Samples for FTIR were maintained at ≤−78 °C after γ-irradiation and transferred into the spectrometer at ≤−60 °C. A "zero-time" spectrum (prior to $PPO_2\cdot$ reaction) was then measured at −60 °C. To eliminate interference ripples from the iPP films, films were inclined at 56° (the Brewster

† Issued as NRCC No. 24877.

0024-9297/85/2218-2092$01.50/0 Published 1985 by the American Chemical Society

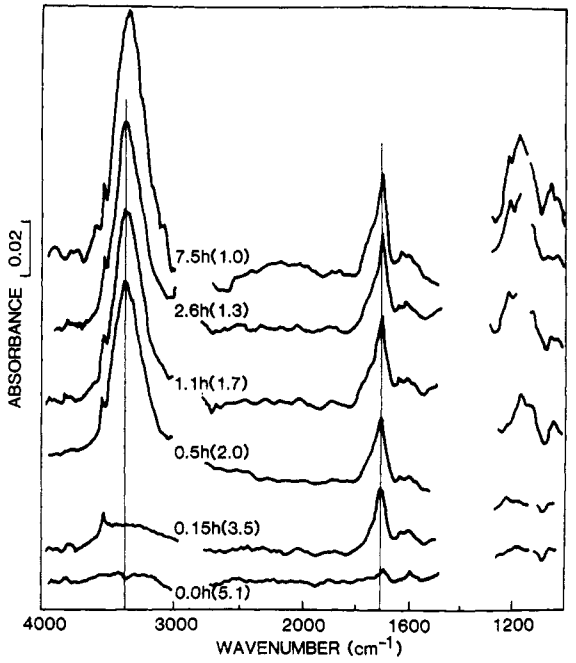

Figure 1. Oxidation product spectra after warming to 23 °C. Difference FTIR spectra were obtained by subtracting the nonoxidized iPP spectrum (five layers, 165-μm optical path) measured under the same conditions as for the oxidized sample. iPP films were γ-irradiated (5 Mrd) in O_2 at −78 °C and then warmed to 23 °C. Values in parentheses are peroxyl radical concentrations ($\times 10^3$, in mol·kg^{-1}) from companion ESR measurements. FTIR and ESR measurements were made after the number of hours shown.

angle) in the polarized IR beam and spectra collected as suggested by Harrick.[9] The NaCl-supported aPP coatings did not generate interference ripples but were complicated by the presence at −60 °C of a broad IR absorption induced by the irradiation of the NaCl support. This IR effect was minimized by subtracting the −60 °C spectrum of an uncoated, but identically irradiated NaCl element using the dedicated FTIR computer. This NaCl absorption was undetectable at 23 °C, although a small interfering absorption persisted at ~3570 cm^{-1}. Spectra of film oxidation products were obtained by subtracting the spectrum of the corresponding unoxidized sample from that of the oxidized sample, both spectra being measured at the same temperature. (Temperature differences caused distinct changes in peak maxima and shapes of the polymer absorptions.) The FTIR spectrometer was a Nicolet 7199, equipped with a broad-band MCT detector operated at 77 K. The addition of 100 spectra at 2-cm^{-1} resolution for each sample usually gave an adequate signal-to-noise ratio.

The FTIR spectra observed for γ-irradiated iPP films after different periods at room temperature (23 °C) are shown in Figure 1, together with the peroxyl concentrations from ESR spectroscopy on identically irradiated and stored film scrolls. These IR and ESR changes are plotted as a function of reaction time at 23 °C in Figure 2. Only changes after 5 Mrd of γ-irradiation in air are presented, although lower doses were also examined, as well as irradiation under vacuum at −78 °C, followed by exposure to O_2 at −78 °C. The latter exposure gave radical and oxidation product yields identical with those for samples irradiated in O_2 or air at −78 °C. This implies that the O_3 always generated during radiolysis in the presence of O_2 plays an insignificant role at this stage of polymer degradation. No oxidation is detected by FTIR prior to warming to 23 °C, consistent with the negligible reactivity of PPO_2· at −78 °C.

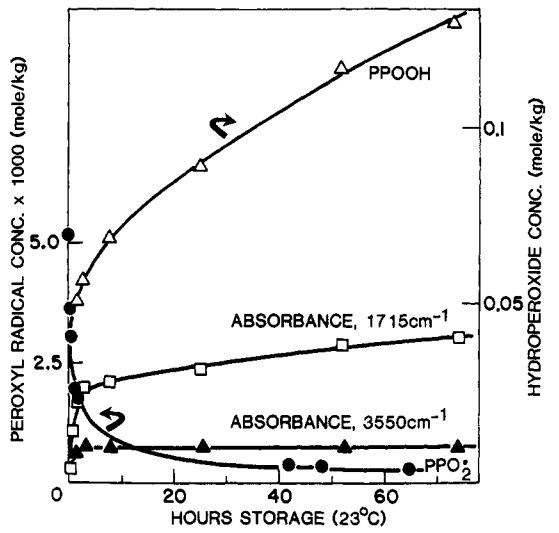

Figure 2. $iPPO_2$· decay and oxidation product accumulation. Experimental conditions as in Figure 1. Maximum absorbances: 0.056 (1715 cm^{-1}); 0.014 (3550 cm^{-1}).

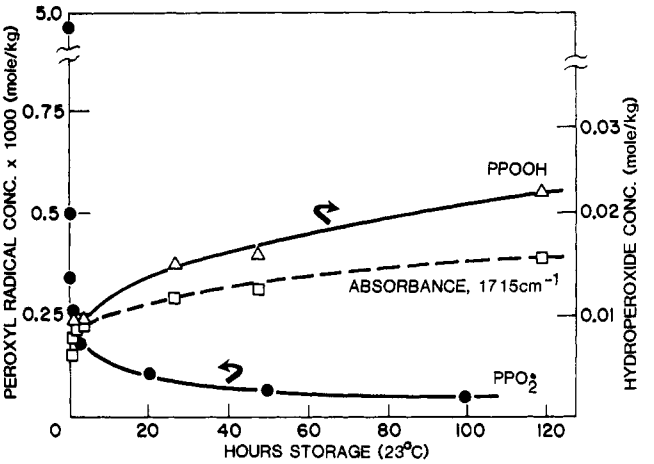

Figure 3. $aPPO_2$ decay and oxidation product accumulation. Experimental conditions as in Figure 1 except that the aPP for FTIR was coated on NaCl as a 140-μm layer. Maximum absorbance: 0.020 (1715 cm^{-1}).

The FTIR spectra contain a wealth of information on the reaction of the peroxyl radical population, although only some features can be unambiguously interpreted.[10] Upon warming to 23 °C, the first products detected are low levels of free (i.e., non-hydrogen bonded) hydroperoxide OH (at 3550 cm^{-1} from comparison with *tert*-butyl hydroperoxide), macroketones (at ~1715 cm^{-1}), and a species absorbing at 1755 cm^{-1}. These are quickly followed by the formation of hydrogen-bonded OH groups at ~3400 cm^{-1}. Hydroperoxide determination by wet chemistry (iodometry) on identically exposed films indicated that ≥90% of the 3400-cm^{-1} absorption resulted from macro OOH groups. (Extinction coefficients for OOH groups were assumed to be 90 cm^{-1}·mol^{-1}·kg for both free and hydrogen-bonded OOH groups and their concentrations calculated from peak heights at 3550 and 3400 cm^{-1}, respectively.) However, the iodometric estimations will also include any of the more unstable peroxides (primary and secondary) which may be formed during PP oxidation (60-min refluxes were required to give plateau levels of iodine generation from γ-irradiated samples). The broad absorbance at ~1150 cm^{-1} is probably indicative of –C–O–. After longer reaction times, the complexity of the carboxyl absorption increases, implying a mixture of acids, peracids, and other species.

In general, similar FTIR changes were found during the decay of aPP peroxyl radicals. Only the time-dependent changes are shown in Figure 3 for aPP. Small, free-hydroperoxide OH (~3550 cm^{-1}) absorptions were again detected in the early stages of $aPPO_2\cdot$ decay, but the low overall level of the OH products (about one-quarter of these from $iPPO_2\cdot$) and overlap with the radiation-modified signal in the NaCl at ~3570 cm^{-1} make quantification of this 3550-cm^{-1} absorbance unreliable.

The initial formation of isolated (non-hydrogen bonded) OOH and ketonic species is consistent with the facile reaction of the radicals formed in each initial peroxyl pair (or clusters of pairs) which result from γ-exposure. The dominant ketonic species probably result from reaction 4b (β-scission of macroalkoxyl radicals) whereas the isolated OOH groups are consistent with the propagation of some of the initial peroxyl radical pairs only once before termination. The dominant oxidation product, hydrogen-bonded OOH groups (3400-cm^{-1} absorption), is believed to result from the extensive intramolecular propagation.[11] The 1755-cm^{-1} band may indicate peracid groups, monomeric (nondimerized) carboxylic acid groups, or (least likely) γ-lactone groups.[12-14] Better, definitive microanalytical tests are needed to distinguish between these species. Peracid and carboxylic acid species imply some attack on the primary C–H sites and/or secondary reactions at C–H groups adjacent to (and so activated by) other oxidation products. In addition, we have no clear information on the formation of peroxide cross-links, which will absorb in the 1150-cm^{-1} region (–C–O– absorption (Figure 1), overlapped with the absorption from hydroperoxide groups).

Although the initial peroxyl concentration is identical in aPP and iPP for a given dose and IR absorptions similar to those in iPP were found in aPP samples as the $aPPO_2\cdot$ population decayed, there are obviously marked differences in product yields as compared to iPP (cf. Figures 2 and 3). Initial peroxyl decay is much faster (6 times) in aPP whereas hydroperoxide and ketone yields are lower (only about one-third) as compared to those in $iPPO_2\cdot$. These differences may result from the greater segmental mobility in aPP, allowing both faster and more efficient radical anihilation reactions presumably to give peroxide, C–C, and C–O–C linkages.

The combined ESR and FTIR data for the $iPPO_2\cdot$ population are consistent with the conclusions that the $PPO_2\cdot$ pairs in the initial and secondary cages self-react rapidly to give some true termination (shown by the very rapid initial drop in $PPO_2\cdot$ concentration) and ketonic species from nonterminating interactions (reactions 3 and 4). The peroxyl radicals which survive the early (predominantly termination) stage do propagate as shown by the OOH formation which continues with progressively increasing kinetic chain length as the $iPPO_2\cdot$ concentration falls. In the first 2 h at 23 °C, each $iPPO_2\cdot$ of the initial population generates on average ~17 hydrogen-bonded OOH groups, ~5 ketonic groups, and ~3 free (isolated) OOH groups, whereas each $aPPO_2\cdot$ yields on average ~6 hydrogen-bonded OOH groups and ~2 ketonic groups (the average extinction coefficient for the center of the ketonic peak envelope at ~1715 cm^{-1} was assumed to be 150 $cm^{-1}\cdot mol^{-1}\cdot kg$).[10] No "free" alcohol OH groups were detected (expected at ~3619 cm^{-1} from model compound studies). For comparison, Decker et al. have implied from G values that each $iPPO_2\cdot$ gave 10 hydroperoxide, 1.4 ketone, 1.0 alcohol, and 0.3 peroxide links whereas $aPPO_2\cdot$ gave 10 hydroperoxide, 1.1 ketone, 1.8 alcohol, and 0.3 peroxide links.[4] However, this latter work depended on product analysis after prolonged oxidation and upon an indirect measure of the concentration of peroxyl radicals generated and was dependent on the assumption that most β-scissions lead immediately to chain termination. Our data clearly contradict this assumption as 4–5 β-scission products are detected for every $iPPO_2\cdot$ lost.

In conclusion, the combined use of FTIR and ESR allows a more complete picture of peroxyl radical self-reactions and propagation to be established. The observed product growth shows that OOH group formation is much faster than $PPO_2\cdot$ decay or macroketone formation, consistent with a classical chain oxidation. The early products, detected as $PPO_2\cdot$ radicals begin to react, point to the predominance of (primary and secondary) cage reactions. These products are consistent with the data of Decker et al., who inferred that a large proportion (~84%) of the initial peroxyl radicals did not propagate but instead reacted together or with other radicals.[3,4] Our yields of β-scission products from the $iPPO_2\cdot$ and $aPPO_2\cdot$ radicals imply that previous evidence of peroxyl radical propagation solely from ESR spectroscopy was complicated by the frequent generation of macroalkyl radicals via the β-scission process, as well as the marked dependence of macroperoxyl radical reactivity upon the history of the radicals.[15]

References and Notes

(1) H. Fischer, K. H. Hellwege, and P. Neudorfl, *J. Polym. Sci., Part A*, 1, 2109 (1963).
(2) B. Eda, K. Nunome, and M. Iwasaki, *J. Polym. Sci., Polym. Lett. Ed.*, 7, 91 (1969).
(3) C. Decker and F. R. Mayo, *J. Polym. Sci., Polym. Chem. Ed.*, 11, 2847 (1973).
(4) C. Decker, F. R. Mayo, and H. Richardson, *J. Polym. Sci., Polym. Chem. Ed.*, 11, 2879 (1973).
(5) D. J. Carlsson, K. H. Chan, A. Garton, and D. M. Wiles, *Pure Appl. Chem.*, **52**, 389 (1980).
(6) J. Reuben and B. H. Mahlman, *J. Phys. Chem.*, 88, 4906 (1984).
(7) S. Shimada, Y. Hori, and H. Kashiwabara, *Macromolecules*, 18, 120 (1985).
(8) K. L. De Vries, R. H. Smith, and B. M. Fanconi, *Polymer*, 21, 949 (1980).
(9) N. J. Harrick, *Appl. Spectrosc.*, 31, 548 (1977).
(10) D. J. Carlsson and D. M. Wiles, *Macromolecules*, 2, 587 (1969).
(11) D. J. Carlsson and D. M. Wiles, *J. Macromol. Sci., Rev. Macromol. Chem.*, **C14**, 65 (1976).
(12) R. D. Mair and R. T. Hall, "Treatise on Analytical Chemistry", Part II, Vol. 14, I. M. Kolthoff and P. J. Elving, Eds., Wiley-Interscience, New York, 1971, p 295.
(13) G. Geuskens and M. S. Kabamba, *Polym. Degrad. Stab.*, 5, 399 (1983).
(14) J. H. Adams, *J. Polym. Sci., Part A-1*, 8, 1279 (1970).
(15) D. J. Carlsson, C. J. B. Dobbin, and D. M. Wiles, *Macromolecules*, in press.
(16) Current address: CIL Inc., Brampton, Ontario, Canada.

D. J. Carlsson,* C. J. B. Dobbin,[16] and D. M. Wiles

Division of Chemistry
National Research Council of Canada
Ottawa, Canada K1A 0R6

Received July 17, 1985